Proceedings of Fifth International Conference on **Enhanced, Compact and Ultra-Compact Heat Exchangers: Science, Engineering and Technology**, Eds. R.K. Shah, M. Ishizuka, T.M. Rudy, and V.V. Wadekar, Engineering Conferences International, Hoboken, NJ, USA, September 2005.

CHE2005 – 66

EFFECT OF CORRUGATION ANGLE ON THE THERMAL BEHAVIOUR OF POWER-LAW FLUIDS DURING A FLOW IN PLATE HEAT EXCHANGERS.

Carla S. Fernandes [(1) (2)], Ricardo P. Dias [(3) (4)], J. M. Nóbrega [(5)], João M. Maia [(6)]

[(1)] *IPC* – Institute for Polymers and Composites, Department of Polymer Engineering, University of Minho, Guimarães, Portugal

[(2)] Mathematics Department, Escola Superior de Tecnologia e de Gestão, Polytechnic Institute of Bragança, Bragança, Portugal; cveiga@ipb.pt

[(3)] Centro de Engenharia Biológica – *IBQF*, University of Minho, Braga, Portugal

[(4)] Chemistry Technology Department, Escola Superior de Tecnologia e de Gestão, Polytechnic Institute of Bragança, Bragança, Portugal; ricardod@ipb.pt

[(5)] *IPC* – Institute for Polymers and Composites, Department of Polymer Engineering, University of Minho, Guimarães, Portugal; mnobrega@dep.uminho.pt

[(6)] *IPC* – Institute for Polymers and Composites, Department of Polymer Engineering, University of Minho, Guimarães, Portugal; jmaia@dep.uminho.pt

ABSTRACT

In this study, CFD calculations were made in order to analyze the thermal behaviour of a power-law fluid in the channels of plate heat exchangers with corrugation angles of 30º and 60º.

For the observed laminar flow, the numerical results show the absence of a typical local temperature profile in the 3D channel. Local Nusselt numbers and transversal variations of viscosity along the plate heat exchangers were studied and simulations considering and discarding the influence of temperature on the non-Newtonian fluid viscosity were performed for the two geometries and the impact of these variations on the thermal correlations was analyzed.

INTRODUCTION

Plate heat exchangers (PHE's) are extensively used in chemical, pharmaceutical, biochemical processing, food, and dairy industries, to name but a few, due to the easy disassembly of the heat exchanger for cleaning and sterilization (Kakaç and Liu, 2002; Gut and Pinto, 2003a, 2003b) and several experimental and modelling works have been performed in order to optimize the design of PHE's leading with Newtonian or non-Newtonian fluids (Bassiouny and Martin, 1984; Gut and Pinto, 2003a, 2003b; Antonini et al., 1987; Leuliet et al., 1987, 1988, 1990; Delplace and Leuliet, 1995; Ciofalo et al., 1996; Mehrabian and Poulter, 2002; Stasiesk et al., 1996; Afonso et al., 2003; Kho and Müller-Steinhagen, 1999; Rao et al., 2002).

Heat transfer in a PHE is strongly dependent on geometrical properties of the chevron plates, namely on corrugation angle, area enlargement factor and channel aspect ratio. Besides these factors, heat transfer is also influenced by the variation of temperature dependent physical properties and especially the variable viscosity effects (Kakaç and Liu, 2002; Metwally and Manglik, 2004; Manglik and Ding, 1997).

When dealing with a non-isothermal flow of a non-Newtonian fluid, the rheological behaviour of the fluid will enhance local variations of physical properties in the PHE (Fernandes et al., 2005). Due to the referred complexity, a general approach is not yet available for problems involving PHE's (Kakaç and Liu, 2002; Manglik and Ding, 1997).

Nusselt numbers are normally described by empirical correlations, being the most common the Dittus-Boetler type (René and Lalande, 1987):

$$\mathrm{Nu} = a\mathrm{Re}^{m}\mathrm{Pr}^{0.3} \tag{1}$$

where a and m are constants dependent on the flow regime and geometrical characteristics of the PHE plates like the corrugation angle. However, when the processed fluids exhibit a strong dependence of viscosity with temperature, the PHE induces changes in velocity fields and normally a Sider & Tate correction is introduced on Dittus-Boetler correlation to describe this effect (René and Lalande, 1987; Antonini et al., 1987):

$$\mathrm{Nu} = a\mathrm{Re}^{m}\mathrm{Pr}^{0.3}\left(\frac{\eta}{\eta_w}\right)^{0.14}. \tag{2}$$

The present study will be focused on numerical simulations of the thermal behaviour of a power-law fluid on the channels of commonly used PHE's.

NOMENCLATURE

a	parameter (-)
b	distance between plates (m)
C_p	specific heat (J kg^{-1} K^{-1})
D_H	hydraulic diameter (m)
E	activation energy (J mol^{-1})
f	fanning friction factor (-)
k	thermal conductivity (W m^{-1} K^{-1})
K_c	consistency index (Pa s^n)
L	effective length (m)
m	parameter (-)
M_v	volumetric flow rate (m^3 s^{-1})
n	flow behaviour index (-)
Nu	Nusselt number (-)
Pr	Prandtl number (-)
q	heat flux (W m^{-2})
R	ideal gas constant (J mol^{-1} K^{-1})
R^2	correlation factor (-)
Re	Reynolds number (-)
T	absolute temperature (K)
u	mean velocity (m s^{-1})
w	effective width (m)
x	spatial coordinate (m)
y	spatial coordinate (m)
z	spatial coordinate (m)
β	corrugation angle (º)
ϕ	area enlargement factor (-)
$\dot{\gamma}$	shear rate (s^{-1})
$\bar{\dot{\gamma}}$	bulk shear rate (s^{-1})
η	apparent viscosity (Pa s)
ρ	density (kg m^{-3})

Subscripts

f	fluid
w	wall

PROBLEM DESCRIPTION

In the present study is performed the simulation of a power-law fluid heating in different PHE's, being the corrugation angles, β, 30º and 60º.

Mathematical formulation

Mathematically, the problem was described by a set of equations that comprises the governing and constitutive equations. The problem could be divided in two problems of heat conduction in the plates and one of laminar non-isothermal flow inside the channel, the governing equations being Fourier's law, to describe the heat conduction in the plates and the Navier-Stokes equations that include the conservation equations for mass, linear momentum and energy, to describe the flow.

The constitutive model used to describe the thermo-rheological behaviour of the fluid is:

$$\eta(T,\dot{\gamma}) = K_c \dot{\gamma}^{n-1} e^{E/RT} \quad (3)$$

where η is the apparent viscosity (Pa s), $\dot{\gamma}$ the shear rate (s^{-1}), T the absolute temperature (K), E the activation energy (J mol^{-1}), R the ideal gas constant (R = 8.31451 J mol^{-1} K^{-1}), K_c the consistency index (Pa s^n) and n the flow behaviour index (-).

The used rheological parameters were similar to the ones of a cloudy apple juice (Steffe, 1996): K_c = 0.0499 Pa s^n, E/R = 3 065 K, n = 0.5.

Numerical resolution

The problem was numerically solved using the finite element method package POLYFLOW and the simulations were performed using a Dell Workstation PWS530 with 1GB of RAM. A complete description of numerical resolution of the present problem is provided by Fernandes et al. (2005).

Geometrical domain. Simulations were carried out in a 3D geometry constituted by three 3D elements: channel, inferior and superior plates. The construction method of the geometrical domain for a corrugation angle of 30º was based on available characteristics of a Pacetti RS 22 PHE (Fernandes et al., 2005). For β = 60º the method was the same, varying only the corrugation angle. It was admitted that the heat exchanger had a parallel arrangement being consequently the flow simulations carried out in a single channel. Additionally, uniform flow was considered inside each channel and, for this reason, a symmetry axis was established, Fig. 1, simplifying the geometrical domain to half of a channel with length, L, of 0.19 m, width, w, of 0.036 m and plates distance, b, of 0.0026 m.

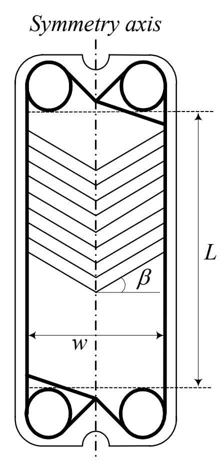

Fig. 1: Schematic representation of a chevron plate.

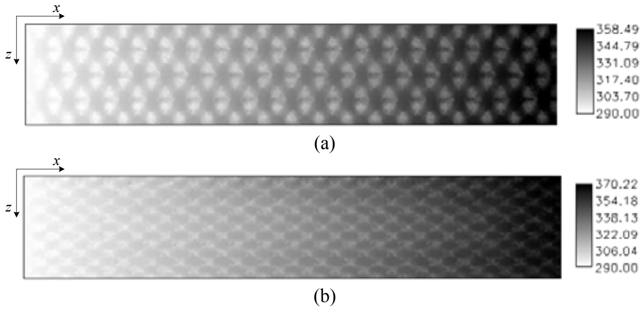

Fig. 2: Temperature distribution along the channel in the plane of contact points (y = 0) for a flow rate 2×10^{-6} m^3 s^{-1} and (a) β = 30º and (b) β = 60º.

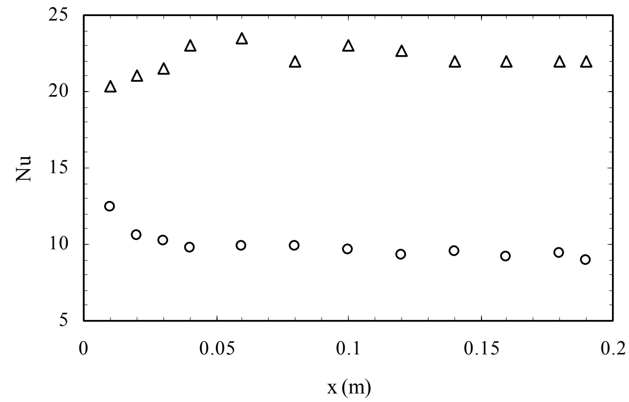

Fig. 4: Local Nussel numbers for the flow rate of 2×10^{-6} m^3 s^{-1} and E/R = 3 065 K for β = 30º (○) and β = 60º (△).

Boundary conditions. A fluid inlet temperature of 290 K was considered in all simulations with different flow rates, having the fluid a thermal conductivity, k, of 0.559 W m^{-1} K^{-1}; specific heat, C_p, of 2 935 J kg^{-1} K^{-1} and density, ρ, of 1 050 kg m^{-3} (Çengel, 1998). A single boundary condition for the different flow rates in the form of a linear heat flux was established along the plates, adapting this way a counterflow general exponential expression to the closest boundary condition allowed by POLYFLOW (Fernandes et al., 2005). In all the simulations slip at the wall and heat losses to the surroundings were assumed to be non-existent.

RESULTS AND DISCUSSION

The number of contact points is largely superior for a corrugation angle of β = 60º. This fact can be observed on Fig. 2 since the contact points are situated on the centre of the darker regions of the referred temperature profiles.

Having the flow a 3D character, elements of fluid with higher temperature, coming from the walls, mix with cold fluid in the bulk, and vice-versa, resulting in the absence of a typical profile for temperature on planes x = *const*. The irregularity of fluid temperature distribution in one of these planes can be observed on Fig.3.

Local distribution of temperature, Fig. 3, allowed average values of fluid, T_f (K) , and wall, T_w (K), temperatures along the channel on planes of equation x = *const*, to be determined.

These temperatures were used in the calculation of local convective heat transfer coefficient, $h(x)$ (W m^{-2} K^{-1}), that can be defined as:

$$h(x) = \frac{q(x)}{(T_f - T_w)(x)}, \tag{4}$$

where $q(x)$ was the heat flux (W m^{-2}) imposed as thermal boundary condition and T_f and T_w were given by POLYFLOW. Consequently, local Nusselt numbers, Nu(x) (-), were determined taking in account the following definition:

$$\mathrm{Nu}(x) = \frac{h(x) D_H}{k}, \tag{5}$$

being D_H (m) the hydraulic diameter (m), defined as $D_H = 2b$.

Fig. 4 represents the local Nusselt numbers for the same flow rate and different corrugation angles. Observing the evolution of Nusselt number it was possible to find a slight oscillatory behaviour which, in turn, is consistent with the continuous x direction sinusoidal behaviour of viscosity, shear stress, temperature and velocity. These local variations were induced by the PHE corrugations (Fernandes et al., 2005).

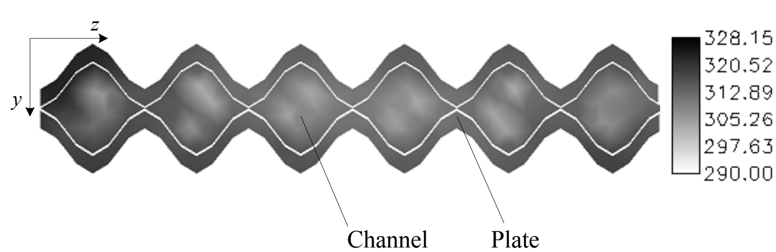

Fig. 3: Temperature distribution in the plane of equation x = 0.09 for the flow rate of 2×10^{-6} m^3 s^{-1}, E/R = 3065 K and β = 60º.

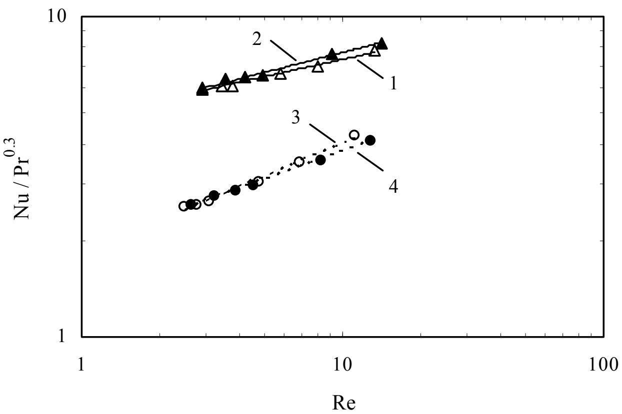

Fig. 5: Thermal correlations for convective heat transfer coefficient for $\beta = 30^o$ and E/R = 3 065 K (◦); $\beta = 30^o$ and E/R = 0 K (•); $\beta = 60^o$ and E/R = 3 065 K (△); $\beta = 60^o$ and E/R = 0 K (▲). 1, 2, 3 and 4 are the fitting lines.

Average values of Nusselt number were calculated for the different flow rates and different PHE's, given raise to the following Dittus-Boetler correlations, Fig. 5:

$$\mathrm{Nu} = 1.809\,\mathrm{Re}^{0.347}\,\mathrm{Pr}^{0.3}\text{ , } R^2 = 0.993 \qquad (6)$$

$$\mathrm{Nu} = 4.859\,\mathrm{Re}^{0.180}\,\mathrm{Pr}^{0.3}\text{ , } R^2 = 0.987 \qquad (7)$$

for β = 30º and β = 60º, respectively, being the dimensionless numbers given by:

$$\mathrm{Re} = \frac{\rho u D_H}{\eta}\text{ ,} \qquad (8)$$

$$\mathrm{Pr} = \frac{C_p \eta}{k} \qquad (9)$$

where the apparent average viscosity was determined by POLYFLOW and average velocity, u (m s^{-1}), was given by:

$$u = \frac{M_v}{wb} \qquad (10)$$

where M_v is the volumetric flow rate (m^3 s^{-1}).

The constant a of Eq. (6) is on good agreement with the value of 1.759 found experimentally by Afonso et al. (2003) with yoghurt, having an n = 0.42, E/R = 11 400 K and being the PHE the simulated on the present work for β = 30º. The same authors found a constant m of 0.455 and refer that this value was obtained due to the high Prandtl numbers (between 581 and 1867) and consequent important entry effects.

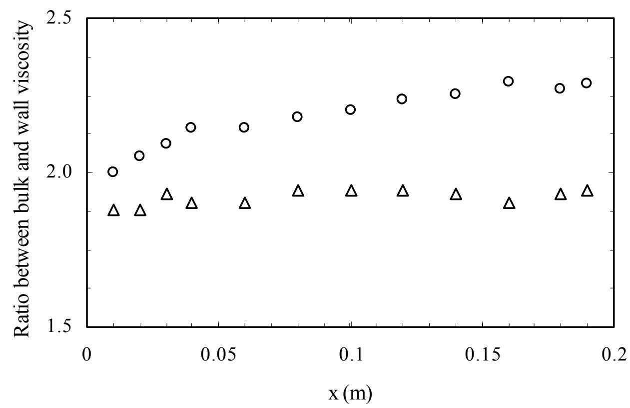

Fig. 6: Ratio between apparent viscosity near the wall and bulk viscosity along the channel with E/R = 3 065 K for flow rate of 2×10^{-6} m^3 s^{-1} and for $\beta = 30^o$ (◦) and $\beta = 60^o$ (△).

On the present work Reynolds numbers are similar (between 2 and 13) to the used by Afonso et al. (2003) but Prandtl numbers are lower (between 45 and 106) and entry effects assumes lower relevance, Fig. 4, conducing to a lower value of m. Although the constant m found in the present work for β = 30º, Eq. (6), being on the typical range for Newtonian fluids (Kakaç and Liu, 2002), for β = 60º, Eq. (7), it was found a value approximately half of that and the constant a increased more than two times when comparing with the present results for β = 30º.

Additionally, simulations disregarding the temperature effect on viscosity (E/R = 0 K) were performed and the following correlations were found:

$$\mathrm{Nu} = 1.924\,\mathrm{Re}^{0.295}\,\mathrm{Pr}^{0.3}\text{ , } R^2 = 0.998 \qquad (11)$$

$$\mathrm{Nu} = 4.772\,\mathrm{Re}^{0.210}\,\mathrm{Pr}^{0.3}\text{ , } R^2 = 0.989 \qquad (12)$$

for β = 30º and β = 60º, respectively. The differences between Eq. (6) and (11), and Eq. (7) and (12) are related with the effect of temperature on axial and transversal viscosity. Simulations with E/R = 0 K have the advantage of providing a lower CPU time and maximum deviation on the Nusselt number between the two cases, for the same flow rate, is lower than 12%.

Since a laminar a flow was observed and due to the presence of important axial and tranversal variations of fluid viscosity, a correction of Sieder & Tate (René and Lalande, 1987; Antonini et al., 1987) on the Dittus- Boetler correlation was included in the analysis.

The ratio (η/η_w) was analysed along the PHE for the two corrugation angles, Fig. 6, being observed that for β = 60º this ratio as an increase tendency along the PHE while for β = 30º remains essentially constant. The already referred oscillatory behaviour can also be observed in the same figure.

For the case where the effect of temperature on viscosity was tacking in account and considering that the temperature of the fluid at the wall is equal to the wall temperature, (η/η_w) is given by:

$$\frac{\eta}{\eta_w}=\left(\frac{\dot{\gamma}_w}{\bar{\dot{\gamma}}}\right)^{1-n}\exp\left(\frac{E(T_w-T_f)}{RT_w T_f}\right) \quad (13)$$

where η_w (Pa s) is the apparent viscosity near the wall, $\bar{\dot{\gamma}}$ the bulk shear rate (s^{-1}), $\dot{\gamma}_w$ the wall shear rate (s^{-1}), being all given by the CFD calculations. When E/R = 0 K, Eq. (13) took the form:

$$\frac{\eta}{\eta_w}=\left(\frac{\dot{\gamma}_w}{\bar{\dot{\gamma}}}\right)^{1-n}. \quad (14)$$

For each Reynolds number, Fig. 7, average values of (η/η_w) on the channel were calculated, and for E/R = 3 065 K the following correlations were found:

$$\mathrm{Nu}=1.602\,\mathrm{Re}^{0.353}\,\mathrm{Pr}^{0.3}\left(\frac{\eta}{\eta_w}\right)^{0.14},\ R^2=0.993 \quad (15)$$

$$\mathrm{Nu}=4.458\,\mathrm{Re}^{0.178}\,\mathrm{Pr}^{0.3}\left(\frac{\eta}{\eta_w}\right)^{0.14},\ R^2=0.985 \quad (16)$$

for β = 30º and β = 60º, respectively. Comparing these correlations, with Eq. (6) and (7) it can be observed that *m* don't suffer big changes while the constant *a* decreases, as expected.

For E/R = 0 K where obtained the correlations:

$$\mathrm{Nu}=1.772\,\mathrm{Re}^{0.295}\,\mathrm{Pr}^{0.3}\left(\frac{\eta}{\eta_w}\right)^{0.14},\ R^2=0.998 \quad (17)$$

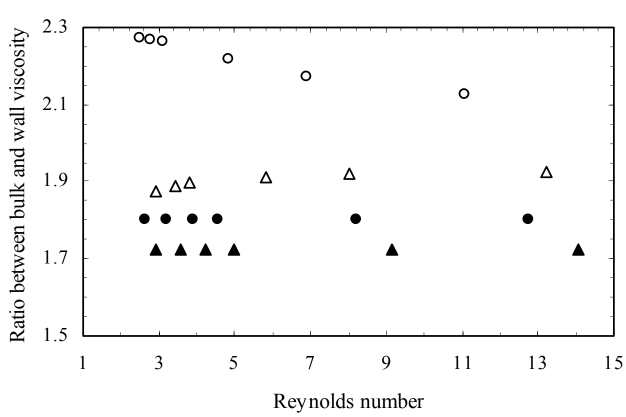

Fig. 7: Ratio between apparent viscosity near the wall and bulk viscosity for different Reynolds numbers for β = 30º and E/R = 3 065 K (○); β = 30º and E/R = 0 K (●); β = 60º and E/R = 3 065 K (△); β = 60º and E/R = 0 K (▲).

$$\mathrm{Nu}=4.423\,\mathrm{Re}^{0.210}\,\mathrm{Pr}^{0.3}\left(\frac{\eta}{\eta_w}\right)^{0.14},\ R^2=0.989 \quad (18)$$

for β = 30º and β = 60º, respectively. Comparing the latter correlations, with Eq. (11) and (12) it can be observed that *m* don't suffer any changes, due to the constant behaviour of the ratio between bulk and wall viscosity for the different Reynolds numbers, Fig. 7, while the constant *a* decreases .

Comparing the obtained Nusselt numbers for the different corrugation angles, for β = 60º they are about two times the obtained for β = 30º for the same flow rate since for the same projected area the area enlargement factor is 1.096 for β = 30º and 1.446 for β = 60º. The shear thinning effect, higher for β = 30º, seems to be the explanation for the higher Nusselt numbers when comparing the present results with Newtonian fluids.

CONCLUSIONS

For the present power-law fluid and operating conditions no typical temperature profile was found along the different corrugation angles PHE's, due to a mixing effect between hot and cold elements of fluid induced by the 3D flow.

Simulations considering the influence of temperature on viscosity and discarding this effect conduced to different thermal correlations and different ratios between bulk and wall viscosities being this ratio higher for a corrugation angle of 30º.

The Nusselt numbers were higher for a corrugation angle of 60º and higher than the observed for Newtonian fluids, for both studied corrugation angles, seeming that the latter observation is related with shear thinning behaviour of the present fluid.

REFERENCES

Afonso, I. M., Hes, L., Maia, J. M., and Melo, L. F., 2003. Heat transfer and rheology of stirred yoghurt during cooling in plate heat exchangers, *Journal of Food Engineering*, 57, pp. 179-187.

Antonini, G., François, O., and Shuai, X. S.,1987. Corrélations transfert/facteur de frottement por le chauffage/refroidissement d'un fluide visqueux à forte dépendance thermorhéologique en écoulement de conduite en régime laminaire, *Revue Générale de Thermique*, 308-309, pp. 427-431.

Bassiouny, M. K., and Martin, H., 1984. Flow distribution and pressure drop in plate heat exchangers – I, *Chemical Engineering Science*, Vol. 39, No. 4, pp. 693-700.

Çengel, Y. A., 1998, *Heat transfer: a pratical approach*, WBC/McGraw-Hill Companies, International Edition.

Ciofalo, M., Stasiek, J., and Collins, M. W., 1996. Investigation of flow and heat transfer in corrugated passages – II. Numerical simulation, *Int. J. Heat Mass Transfer*, 39, pp.165-192.

Fernandes, C. S., Dias, R., Nóbrega, J. M., Afonso, I. M., Melo, L. F., and Maia, J. M., 2005. Simulation of stirred yoghurt processing in plate heat exchangers, *Journal of Food Engineering*, 69, pp. 281-290.

Gut, J. A. W., and Pinto, J. M., 2003a. Selecting optimal configurations for multisection plate heat exchangers in pasteurization processes, *Ind. Eng. Chem. Res.*, 42, pp. 6112-6124.

Gut, J. A. W., and Pinto, J. M. 2003b. Modeling of plate heat exchangers with generalized configurations, *International Journal of Heat and Mass Transfer*, 46, pp. 2571-2585.

Kakaç, S., and Liu, H., 2002. *Heat exchangers selection, rating, and thermal design*, 2nd ed., CRC Press, Boca Raton.

Kho, T., and Müller-Steinhagen, 1999. An experimental and numerical investigation of plate heat transfer fouling and fluid flow in flat plate heat exchangers, *Trans IChemE*, Vol 77, Part A, pp. 124 – 130.

Leuliet, J. C., Maigonnat, J. F., and Lalande, M., 1987. Etude de la perte de charge dans de échangeurs de chaleur à plaques traitant des produits non-newtoniens, *Rev. Gén. Therm. Fr.*, 308-309, pp. 445-450.

Leuliet, J. C., Maigonnat, J. F., and Lalande, M., 1988. Thermal behaviour of plate heat exchangers with Newtonian and non-Newtonian fluids, *Congrés Eurotherm 5 et 1er Colloque TIFAN*, Compiègne, France.

Leuliet, J. C., Maigonnat, J. F., and Lalande, M., 1990. Écoulement et transferts de chaleur dans les échangeurs à plaques traitant des produits visqueux newtoniens et pseudoplastiques, *The Canadian Journal of Chemical Engineering*, 68, pp. 220-229.

Manglick, R. M., and Ding, J., 1997. Laminar flow heat transfer to viscous power-law fluids in double-sine ducts, *International Journal of Heat and Mass Transfer*, Vol. 40, No. 6, pp. 1379-1390.

Mehrabian, M. A., and Poulter, R., 2000. Hydrodynamics and thermal characteristics of corrugated channels: computacional approach, *Applied Mathematical Modelling*, 24, pp. 343-364.

Metwally, H. M., & Manglick, R. M., 2004. Enhanced heat transfer due to curvature-induced lateral vortices in laminar flows in sinusoidal corrugated-plate channels, *International Journal of Heat and Mass Transfer*, 47, pp. 2283-2292.

Rao, B.P., Kumar, P.K., and Das S. K., 2002. Effect of flow distribution to the channels on the thermal performance of a plate heat exchanger, *Chemical Engineering and Processing*, 41, pp. 49-58.

René, F., and Lalande, M., 1987. Échangeur de chaleur à plaques et joints. Résolution numérique des équations d'échange thermique entre les différents canaux, *Revue Générale de Thermique*, 311, pp. 577-583.

Stasiek, J., Collins, M. W., Ciofalo, M., and Chew, P. E., 1996. Investigation of flow and heat transfer in corrugated passages – I, Experimental results, *Int. J. Heat Mass Transfer*, 39, pp. 149-164.

Steffe, J. F., 1996, *Rheological methods in food process engineering*, 2nd ed., Freeman Press, East Lansing.